



Mild pyrolysis of cotton coated with graphene-like materials as a method to produce superhydrophobic and highly absorptive oil sorbents

Damian Łukawski¹ · Małgorzata Widelicka² · Anna Martin¹ · Filip Lisiecki² · Alina Dudkowiak¹

Received: 1 November 2022 / Accepted: 4 July 2023 / Published online: 19 July 2023
© The Author(s) 2023

Abstract

In recent years, hydrophobized cellulose-based materials have been proposed as oil spill sorbents. We investigate the possibility of using cheap, industrialgrade, graphene-like materials (GM), such as graphite flakes (GrF), exfoliated graphene nanoplatelets (xGNP) and microwave-plasma turbostratic graphene nanoplatelets (mGNP) as hydrophobic agents for naturally hydrophilic cotton. From among investigated GM, mGNP showed the highest ability to form superhydrophobic coating due to small flake size and small amount of impurities. Furthermore, we showed that mild pyrolysis not only makes cotton more hydrophobic, but also increases its sorption capacity towards organic solvents and oils. Pyrolyzed and coated with mGNP and xGNP cotton showed exceptional superhydrophobic properties and water contact angle equal 148° and 142°, respectively, besides the sorption capacity towards motor oil of 46 g/g and 51 g/g, respectively. What is more important, the price of graphene oxide used in previous research is still very high (approx. 100 \$/g), while the price of xGNP and mGNP is 0.45 \$/g, 7.3 \$/g, respectively. This difference may be crucial for the implementation of graphene-based sorbents in the remediation of massive oil spill remediation.

Keywords Cotton · Graphene nanoplatelets · Oil spill · Pyrolysis · Sorbent

Introduction

The significant impact of oil spills has prompted extensive research into effective methods of their removal. One such methods involves the use of sorbents that can remove or prevent further spread of oil (Oliveira et al. 2021). To be effective, these sorbents should be hydrophobic or superhydrophobic to selectively absorb oil without absorbing water. In addition, properly designed selective sorbents should possess high sorption capacity (SC), chemical stability, and environmental friendliness (Gupta and Tai 2016).

Graphene-coated materials have emerged as potential superhydrophobic oil spill sorbent. Its superhydrophobic

behavior is caused by its high surface area, low surface energy, and the hierarchical structures formed by the edges and defects of the graphene sheets. The combination of these factors leads to a high water contact angle and a low sliding angle of water droplets on the graphene surface. Several studies have investigated the superhydrophobic properties of graphene and its derivatives, and a comprehensive understanding of the underlying mechanisms has been established (Kim et al. 2022; Wang et al. 2015; Belyaeva and Schneider 2020).

Graphene-based aerogels and foams have been suggested for oil removal (Lin et al. 2011; Dong et al. 2012; Singh et al. 2013; Xu et al. 2015; Li et al. 2014; Ha et al. 2015). However, the relatively high cost of these sorbents may present a significant challenge for their widespread use in the event of large-scale ocean oil spills.

Another approach to remove oil spills involves the creation of graphene/polymer sponges, which exhibit high sorption capacity and reusability. This strategy involves utilizing polymers to construct a three-dimensional structure and incorporating graphene to impart hydrophobicity (Cho et al. 2015; Saha and Dashairya 2018; Ji et al. 2017). The

✉ Damian Łukawski
damian.lukawski@put.poznan.pl

¹ Faculty of Materials Engineering and Technical Physics, Poznan University of Technology, Piotrowo 3, 60-965 Poznan, Poland

² Institute of Molecular Physics, Polish Academy of Sciences, Smoluchowskiego 17, 60-179 Poznan, Poland

deposition of graphene can be achieved through two distinct methods. In the first approach, graphene oxide (GO) is first deposited from aqueous suspension and then transformed into reduced graphene oxide (rGO) on the polymer sponge (Saha and Dashairya 2018; Nguyen et al. 2012; Shiu et al. 2018). The second method involves the direct deposition of rGO or graphene nanoplatelets (GNP) onto polymer sponge (Cho et al. 2015; Su et al. 2017; Lv et al. 2015a). Although synthetic polymers exhibit desirable sorption capacity and cost-effectiveness, their use may be restricted due to their non-biodegradability. Therefore, efforts have been made to deposit graphene onto sponges made of biopolymers, such as lignin or cellulose.

Lignin-based polyurethane composed of octadecylamine and covered with rGO has also been used as a hydrophobic sponge (Oribayo et al. 2017). Cotton is a readily available, low-cost, highly sorptive, and biodegradable material, but due to its natural hydrophilicity, it requires hydrophobization. A common approach is to coat cotton with polymethylsiloxane (Shateri-Khalilabad and Yazdanshenas 2013) results in superhydrophobic cotton sorbents. Alternatively, graphene-like materials (GM), such as graphene oxide (GO), can be used to hydrophobize cotton sorbents. Several studies have explored the use of GM/cotton sorbents (Shateri-Khalilabad and Yazdanshenas 2013; Ge et al. 2014; Hoai et al. 2016; Tissera et al. 2015; Cai et al. 2017). However, studies have focused on water-soluble GO, which is naturally rather hydrophilic and, therefore, requires thermal (Cai et al. 2017) or hydrothermal (Ge et al. 2014) modification to obtain hydrophobic properties. In addition, GO is still very expensive, in comparison with commercially available GNP or graphite flakes (GrF).

The utilisation of GNP or even GrF, instead of GO, presents significant advantages for the cost-effective and efficient production of hydrophobic sorbents. A multi-layered graphene may be produced by chemical exfoliation of graphite (Shen et al. 2009; Viculis et al. 2005) and microwave-plasma method (Malesevic et al. 2008) or other plasma enhanced methods (Bo et al. 2013). Only a few studies (Kugler et al. 2015; Łukawski et al. 2018a, 2018b) have described the use of GNP or microwave plasma graphene

(Łukawski et al. 2018b). instead of GO or rGO as hydrophobic agent. Yet, no comparison of various types of GM, having various sizes and defects, has been made in terms of the hydrophobization surface of cotton to be used as selective sorbent. In this paper we compared microwave-plasma GNP (mGNP), chemically exfoliated GNP (xGNP) and GrF, as hydrophobic agents used on cotton sorbents. In addition, we propose the use of mild pyrolysis on GM-coated cotton sorbents. Mild pyrolysis has been earlier investigated by Y. Kato et al. (Kato et al. 1997a) as the method of increasing both hydrophobic properties and sorption of oils by of wood fibers. Applying this process to GM coated cotton may create superhydrophobic and highly efficient sorbent.

Experimental

Materials

The study was performed on commercially available and produced on large-scale GNP and GrF. GrF (average diameter < 45 μm) powder purchased from Herbaviridis, xGNP produced by Cheap Tubes Inc. (average diameter 25 μm), and mGNP from Cambridge Nanosystems (average diameter 0.4 μm). To obtain hydrophobic xGNP powder, the pristine xGNP powder was placed in vacuum oven for 12 h in 250 $^{\circ}\text{C}$ before deposition onto cotton.

The cotton fabrics used as the sorbent frame were degreased cotton roving (Sigma Aldrich, BRAND[®] cotton roving, density approx. 1.3 g per 1 m). Dichloromethane (DCM) (spectroscopy grade) used for dispersion preparation, and hexane (petroleum fraction), chloroform, and ethanol for sorption tests were purchased from Avantor Performance Materials Poland SA. Motor oil (SAE 30) and diesel oil were purchased from local suppliers.

Preparation of sorbents

The GM/cotton sorbents were prepared, as shown in Fig. 1. GM were dispersed by Hielsher 400 St ultrasonic horn for 10 min, using sonication power 40 W per 40 ml. They were

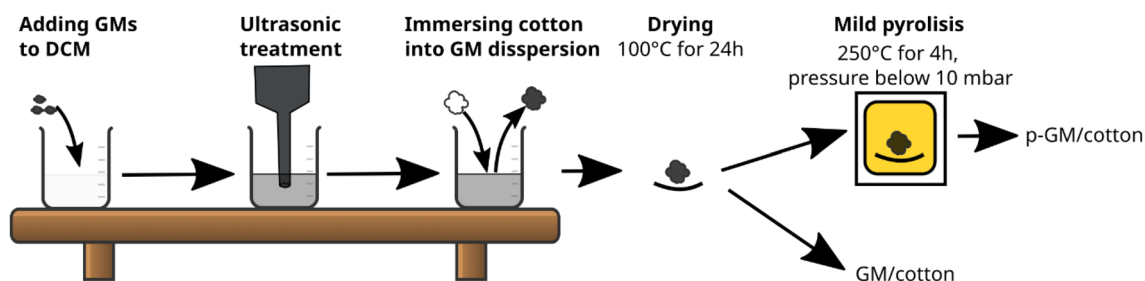


Fig. 1 Schematic process of hydrophobic sorbent preparation

prepared in DCM at a concentration of 1 mg/1 ml. DCM was chosen as an organic solvent because of its very high vapour pressure. Pure cotton roving pieces were dried in 100 °C for 24 h to remove moisture and weight (the samples with final mass varying from 28 to 32 mg were chosen). Then, samples were immersed in GM dispersions and dried. The procedure was repeated three times and before each dip-coating, the dispersion was sonified in ultrasonic bath for 1 min to avoid GM agglomeration. Finally, tests were performed for samples after layer by layer deposition repeated three times. Afterwards, all samples were dried at 100 °C for 24 h and weighted. Some of the samples were then pyrolyzed in a vacuum oven (below 10 mbar) for 4 h in 250 °C.

Characterization of samples

GM powers were initially investigated by thermogravimetric analysis (TGA) which was performed on Perkin Elmer 4000 with the heating rate set to 10 °C/min in nitrogen atmosphere and Brunauer–Emmett–Teller (BET) surface area was estimated by the High Throughput Analysis System (ASAP 2420 Micromeritics). GM were degassed in 300 °C before BET test. The Raman spectra were collected with a Jobin Horiba LabRAM HR 800 spectrometer connected with a CCD detector, in 1200–1800 cm^{-1} and 2400–2800 cm^{-1} range. For measurements the He–Ne laser excitation line 633 nm was used. Scanning electron microscopy (SEM) images were taken with a FEI Nova NanoSEM 650 microscope, and energy-dispersive X-ray spectroscopy (EDS) measurements were performed using a Bruker XFlash® 5010 detector (please see Supplementary Materials).

Contact angle (θ) was measured with a CCD camera (Nikon D300s). Droplets of $10.0 \pm 0.5 \mu\text{l}$ were deposited using a Hamilton microsyringe (25 μl). The water droplet volume was increased with respect to its size in the standard contact angle measurements because of the very high roughness of cotton. The θ angles were measured on each surface four times with the aid of the Dropsnake plugin to ImageJ software (Stalder et al. 2006) and the results are presented as mean values with standard deviation.

The stability assessment of the coatings was based on the comparative analysis of the sorption capacity of samples under controlled laboratory conditions and after exposure to solar irradiation and high levels of atmospheric humidity. Sun 3000 Solar Simulators from Abet Technologies was employed to subject the coatings to an illumination intensity comparable to 24 h of natural sunlight. To determine the effect of humidity on the sorption properties of the coatings, samples were placed in a closed humidity chamber for 24 h, where the relative humidity of the air was $(87 \pm 3)\%$.

Sorption measurements

The samples were immersed in deionised water for 10 s, followed by leaching for 10 s leaching. The saturation measurements were made for five samples. The results presented were the averages of all measurements, and the standard deviation was calculated as measurement uncertainty. SC was calculated from the following formula:

$$SC = \frac{m_f - m_0}{m_0} \quad (1)$$

where m_f is the mass of sample after immersion in fluid, m_0 is the initial mass of sample.

SC measurements were performed with the exact procedure for organic solvents. SC of each fluid was measured for three samples.

The recyclability measurements were performed by repeating vacuum filtration of sorbents soaked with ethanol. Vacuum filtration was performed at room temperature in a pressure from below 10 mbar for 1 h. SC was measured as described above, and collection capacity (CC) was measured by weighing the sample after vacuum filtration and calculated from the formula:

$$CC = \frac{m_1 - m_0}{m_0} \quad (2)$$

where m_1 is the mass of sample after vacuum filtration.

Results and discussion

Industrial grade GM as potential hydrophobic agents

Three types of GM were investigated as potential hydrophobic agents. GrF shows the highest average flake size ($\sim 45 \mu\text{m}$) and the lowest BET specific surface area ($6.5 \text{ m}^2/\text{g}$). In addition, two types of xGNP with an average size of 5 μm and 25 μm and small mGNP (average diameter 400 nm). The BET specific surface areas of xGNP and mGNP are similar and exceed $125 \text{ m}^2/\text{g}$ (see Supplementary Materials, Table S1). All GM powders form agglomerated structures before ultrasonic treatment. From among the selected samples, mGNP shows an outstanding sponge-like structure made of small and wrinkled flakes (Fig. 2). TGA results (Fig. 2d) indicate that mGNP and GrF were thermally stable to 600 °C, but both xGNP were stable only to 400 °C, which could be caused by partial GO-like residues. However, in comparison with xGNP, pure GO is stable only to 200–250 °C (Some et al. 2013).

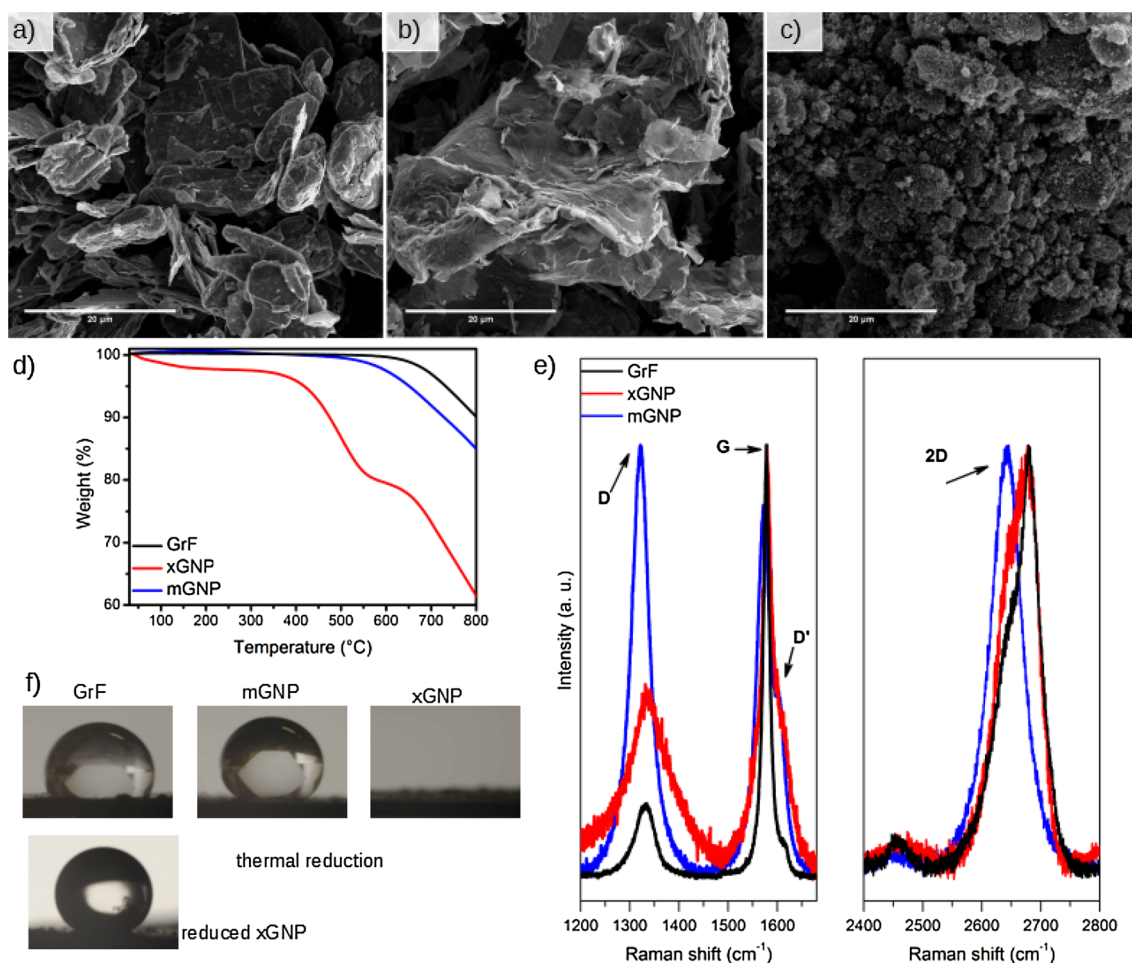


Fig. 2 Characterisation of GM powders. SEM images of GrF **a** xGNP **b** mGNP **c** TGA **d** Raman spectra **e** water contact angle (θ) **f**

The Raman spectra of the investigated GM revealed characteristic graphene bands D, G, D' and 2D (Fig. 2e). Peak G ($\sim 1580\text{ cm}^{-1}$) was visible in the Raman spectrum of each GM. Peak D ($\sim 1330\text{ cm}^{-1}$) corresponded to the breathing modes of carbon rings, which were activated in the presence of defects and edges. Peak 2D ($\sim 2680\text{ cm}^{-1}$) is an overtone of peak D and a result of the two-phonon process with opposite wave vectors. Due to its origin, no defects are required in its activation (Ferrari and Basko 2013). For samples GrF and xGNP peak 2D comprises many components, the maximum of band 2D is located at around $\sim 2685\text{ cm}^{-1}$. Several components of band 2D indicate that many graphene layers were investigated during the experiment. For mGNP sample, this peak is symmetric and situated at lower energies ($\sim 2640\text{ cm}^{-1}$), which is typical of turbostratic layered graphene (Ferrari et al. 2006; Rytel et al. 2018).

The nature of defects was analysed on the basis of the ratio of integral intensities of the peaks D and D' (AD/AD'). Such an approach has been used in previous works (Rytel

et al. 2018; Eckmann et al. 2012). Peak D' ($\sim 1610\text{ cm}^{-1}$), caused by the double resonance intra-valley processes of zone-boundary phonons, is an overtone of peak D and occurs in defective samples. For xGNP, the ratio AD/AD' equals 5.9, which can correspond to the presence of both edge and vacancy defects. For the mGNP sample, this ratio equals 7, which corresponds to vacancy defects, only. The highest value of AD/AD' equals 9.3 for sample GrF and indicates the presence of sp^3 hybridization defects in this material. After their initial characterization, GM powders were investigated in terms of wetting (Fig. 2f). As expected, the highest θ angle and superhydrophobic behavior was observed for mGNP ($142^\circ \pm 2^\circ$), due to its smallest flake size and in consequence higher nanoscale surface roughness. The θ angle of GrF was slightly lower ($114^\circ \pm 5^\circ$), but the surface was still hydrophobic. However, xGNP showed complete wettability with θ angle equal 0° . This observation can be explained by the presence of edge defect observed in Raman spectra. These edge defects may be functionalised by $C=O$ or $-COOH$ groups, responsible for hydrophilic properties.

An additional EDS measurement was performed to detect other, not related to oxygen, that may cause the hydrophilic character of the xGNP powder (Fig. 2f). In comparison with GrF and mGNP, which were hydrophobic, the EDS spectra of xGNP show a very strong sulphur signal at 2.3 keV (please see Supplementary Materials Fig. S1 a). The presence of sulphur may be the key factor in understanding the wetting properties of GNP. Its presence is probably related to residual sulfuric acid or sulfonic/thiol groups attached to xGNP, left during chemical exfoliation. These groups are supposed to be responsible for the hydrophilic properties of xGNP.

However, sulfur-containing groups is removed during ultrasonic treatment in DCM and deposition onto cotton (please see Supplementary Materials, Fig. S1b). To remove the other hydrophilic contaminants, xGNPs were additionally thermally reduced under vacuum at 250 °C for 12 h. The reduction process caused a rapid increase in θ angle to $143 \pm 3^\circ$ (Fig. 2f). All subsequent experiments were performed with reduced xGNP.

Wetting of GM/cotton and pyrolyzed GM/cotton

Cotton roving was used as a biopolymer sorbent due to very high sorption capacity, low price and biodegradability. However, raw cellulose, the sole component of degreased cotton roving, is highly hydrophilic and needs to be properly hydrophobized to be applied as an oil spill sorbent. Studies performed by Kato et al. 1997b on wood fibers, revealed a significant water repellent properties after mild pyrolysis. In this research we proposed a similar approach on cotton roving to decrease its hydrophilicity.

It is well-known that cellulose is rich in hydroxyl groups that are prone to be wet by water. The recorded FTIR

spectra (Fig. 3) of cotton roving were typical characteristic absorptions for cellulose that have been described many times before (Ciolacu et al. 2011; Lv et al. 2015b). The IR absorption peaks appeared around 3340 cm^{-1} (OH stretching), 2900 cm^{-1} (CH_2 stretching; CH stretching), 1630 cm^{-1} (adsorbed H_2O), 1435 cm^{-1} (CH bending), 1370 cm^{-1} (CH bending and COO stretching), 1320 cm^{-1} (CH bending and OH bending), 1165 cm^{-1} (C–O–C in bridge, asymmetric stretching), 1103 cm^{-1} (ring valence vibration), 1050 cm^{-1} (O–C–O stretching). The mild pyrolysis in 250 °C did not significantly influence the FTIR spectra. No shifts of the main peaks are observed, while the differences in intensities of individual peaks may be caused by differences in morphology of pellets. However, an additional peak at 1725 cm^{-1} (Fig. 3 insert), attributed to C=O absorption, appeared. According to Lv et al. (2012) this indicates the formation of indicating the formation of ketones or aldehydes. Furthermore, according to the findings presented by Arsenau (Arseneau 1971) and Lv (Lv et al. 2015b) mild cellulose pyrolysis leads to dehydration and possible cleavage of the cellulose structure at 250 °C. In consequence, pyrolyzed cellulose may be characterized by lower wettability than raw cotton. Next, GM/cotton sorbents were prepared according to Sect. "Preparation of sorbents". The camera image showed a homogeneous cotton coating in macroscale and no presence of large-scale agglomerates of mGNP and xGNP, but visible agglomerates of GrF (please see Supplementary Materials, Fig. S2). However, wetting properties are dependent mostly on micro-nano scale quality of coating, so SEM images were recorded for the investigated GM/cotton sorbents (Fig. 4).

It is easily seen that GrF (Fig. 4a) formed heterogeneous coatings on the micro-nano scale. Significantly more uniform was the xGNP coating (Fig. 4b), but the highest homogeneity was observed for mGNP (Fig. 4c).

After SEM characterisation of the GM coatings, sorption measurements were performed. The water contact angle was evaluated for all samples (Table 1). As expected, degreased cotton roving, consisting of pure cellulose fibres, was highly hydrophilic and the droplet of water was immediately soaked up. Similar observations were made for GrF/cotton, attributed to the heterogeneity of the GrF coating visible in the SEM image (Fig. 2a). Unlike GrF/cotton, xGNP/cotton becomes slightly hydrophobic, but significantly higher hydrophobicity is caused by the mGNP coating, characterised by the θ angle of 132° . It is because mGNP formed the most homogeneous coating formed by small flakes (Fig. 2c).

To increase water repellent properties of cellulose fibers and in consequence of the sorbent, the samples were mildly pyrolyzed. Although, the θ angle of pyrolyzed (p-) cotton remained 0° , pGrF/cotton became hydrophobic, with the θ angle equal to 123° . This is due to the synergistic effect of hydrophobization by pyrolysis and GrF coating. The highest

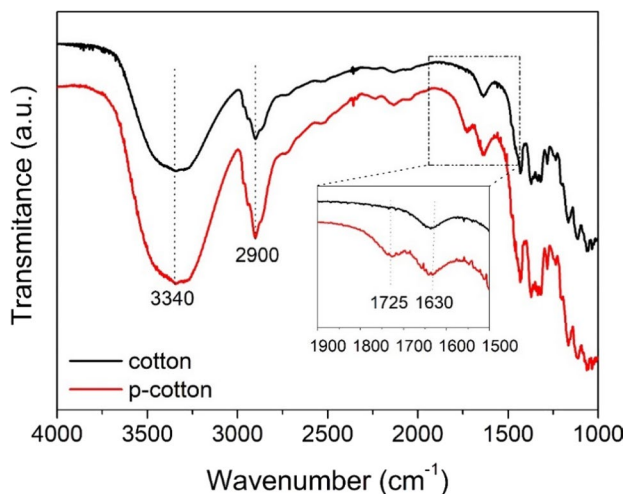


Fig. 3 FTIR spectra of cotton and p-cotton

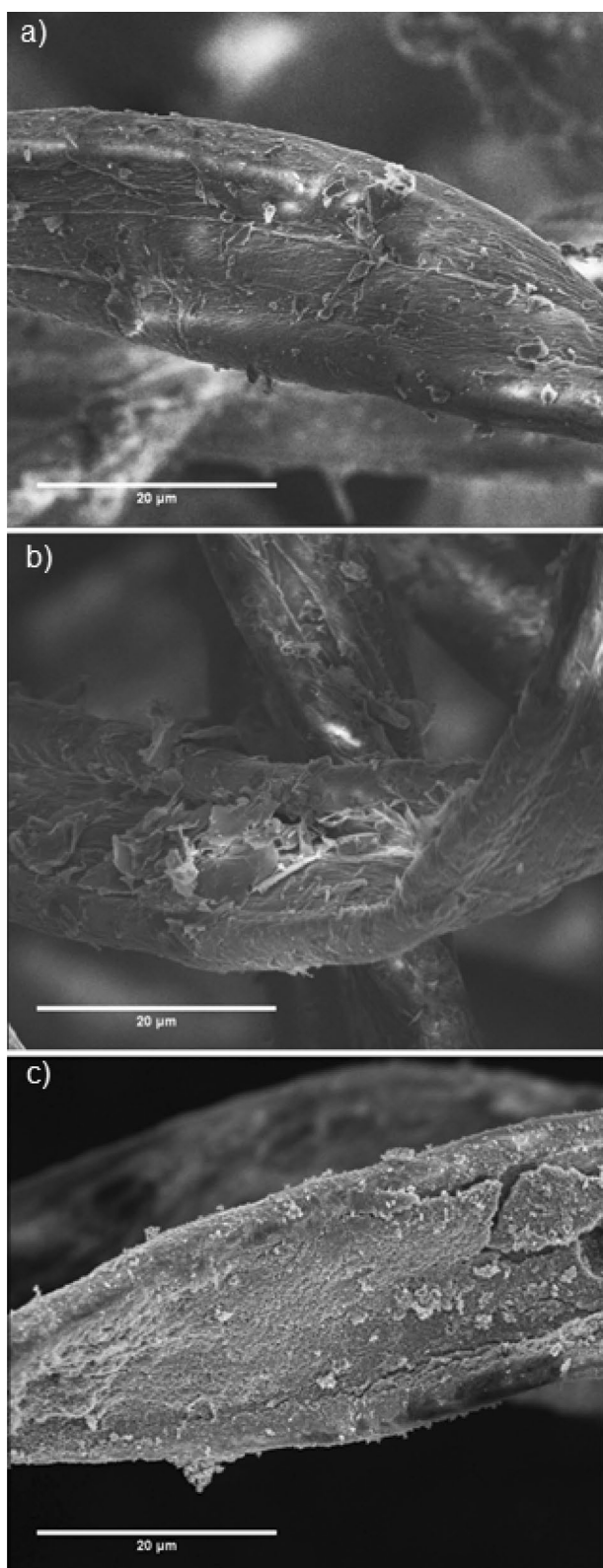


Fig. 4 SEM images of cotton coated with 3 layers of: GrF **a**, xGNP **b**, mGNP **c**

water repellent properties were observed for p-xGNP/cotton and pmGNP/cotton, characterized by the angles of 142° and 148° , respectively.

Water contact angle measurement was followed by measuring sorption capacity (SC) towards water (for image presenting water sorption measurement, please see Supplementary Materials Fig. S3). SC of cotton and p-cotton, GrF/cotton exceeded 40 g/g . The GrF flakes were clearly distributed heterogeneously, which caused the wetting of the uncoated cellulose fibres and the distribution of water through the sorbent by capillary forces (Fig. 5). SC was significantly lower for mGNP/cotton, in which the cotton yarns were covered by a uniform superhydrophobic layer. A slight, but visible water repellent properties were also observed for xGNP/cotton (Table 1).

Large size of xGNP flakes causes their heterogeneous distribution on cellulose fibers and in consequence only partial water repellent properties. Pyrolysis was performed to decrease the wetting of the unprotected cellulose fibers in cotton yarn. Although pyrolysis alone did not cause any significant changes in θ angle or in SC, together with xGNP or mGNP coating it contributed to forming highly water repellent sorbent. In consequence, pxGNP/cotton and pGNP/cotton showed SC below 2 g/g and θ angle exceeding 140° . Finally, due to the highest θ angle and the lowest SC, the samples of p-xGNP/cotton, pmGNP/cotton were chosen for further experiments. As reference samples cotton, p-cotton and superhydrophobic but not pyrolyzed mGNP/cotton were also tested.





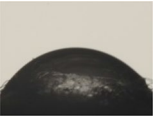

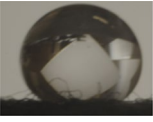
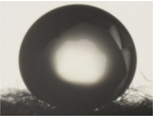
GM/cotton oil sorbents

Superhydrophobic properties of the sorbent are a crucial, but not the only important feature. The sorbent should show high SC towards oils, but also towards organic solvents. The SC of selected samples showing the highest water repellent properties and reference sorbents were evaluated.

Organic liquids such as hexane, ethanol, diesel oil, motor oil and chloroform were investigated. The density of these liquids ranged from 0.65 kg/l to 1.49 kg/l and their dynamic viscosity—from $0.3 \text{ mPa} \times \text{s}$ to $240 \text{ mPa} \times \text{s}$ (for detailed density and dynamic viscosity values, see Supplementary Materials Table S2). The process of motor oil sorption of cotton and mGNP/cotton are presented in Fig. 6.

At first, cotton and p-cotton were investigated (Fig. 7). SC varied from 30.8 g/g to 63 g/g and 45 g/g to 72 g/g , for cotton and p-cotton, respectively. P-cotton showed an average 23% higher SC towards organic liquids, which is probably caused by the expansion of the pores in cellulose fibres during pyrolysis. However, its SC towards water did not increase, which means that partial hydrophobization of cotton occurred.

Table 1 Water contact angle and sorption capacity towards water of various sorbents (standard deviation in parentheses)

Hydrophobic agent	θ (°)		SC (g/g)	
	cotton	pyrolyzed cotton	cotton	pyrolyzed cotton
none	 0	 0	45.2 (1.0)	46.6 (1.5)
GrF	 0	 123 (7)	42.5 (2.4)	32.7 (2.7)
xGNP	 82 (17)	 142 (8)	11.1 (1.2)	1.8 (0.2)
mGNP	 132 (4)	 148 (6)	1.8 (0.5)	0.18 (0.04)

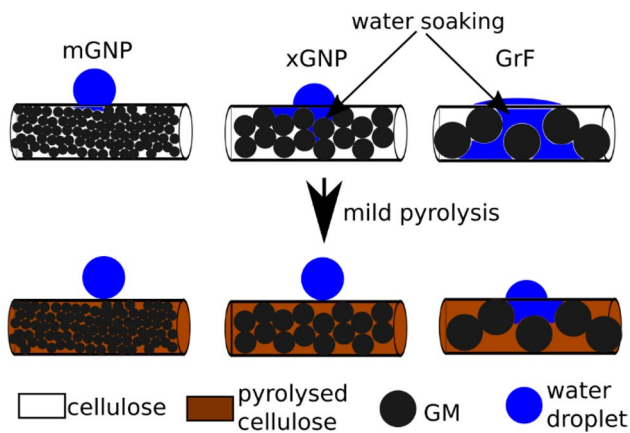


Fig. 5 Model of water sorption by GM hydrophobized and pyrolyzed cotton

After coating with mGNP, the cotton sorbents became highly water repellent (SC towards water equal 1.8 g/g) and only slightly less absorptive towards organic liquids, with the highest SC varying from 28.7 g/g to 49.7 g/g, for hexane and chloroform, respectively. After pyrolysis of p-mGNP/cotton it showed higher SC towards hexane, ethanol, diesel oil and chloroform (30.7 g/g to 59.6 g/g, for hexane and chloroform, respectively), and SC towards motor oil similar to that of mGNP/cotton. Slightly lower SC values (30.5 g/g to 53.6 g/g, for hexane and chloroform, respectively) were obtained for p-xGNP/cotton. In general, each sorbent showed the highest SC towards



Fig. 6 Motor oil sorption by cotton (top) and mGNP/cotton (bottom) sorbents

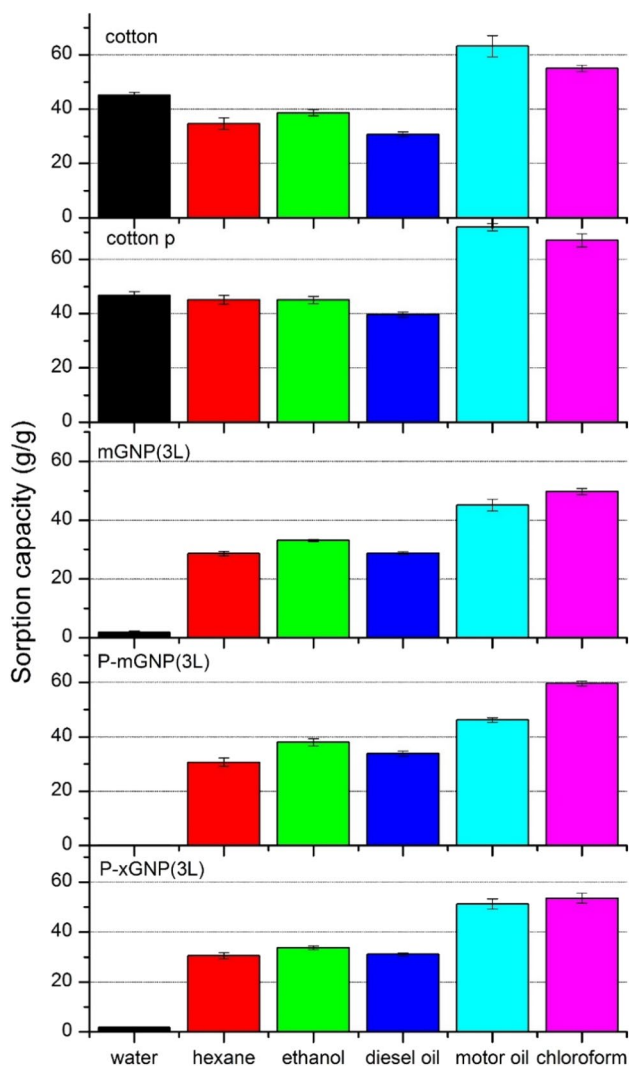


Fig. 7 Sorption capacity towards water, hexane, ethanol, diesel oil, motor oil and chloroform of various sorbents

chloroform (due to its highest density) and motor oil (due to its highest viscosity), while the lowest SC towards hexane (due to its lowest viscosity and density).

The sorption capacity is the most important parameter, but the soaking rate is also important in some situations. Therefore, sorption kinetics towards motor oil and chloroform was tested for reference (cotton), pyrolyzed (p-cotton) graphene-coated (mGNP/cotton) and pyrolyzed and graphene coated (p-mGNP/cotton) to understand the influence of all modifications on the sorption rate. Due to the very low viscosity, the results for chloroform showed a rapid increase in SC and after 1 s almost 100% of maximum SC was reached (please see, Supplementary Materials Fig. S4a). No significant changes in the sorption rate were observed among the four tested samples. For motor oil the sorption speed was not high as for chloroform,

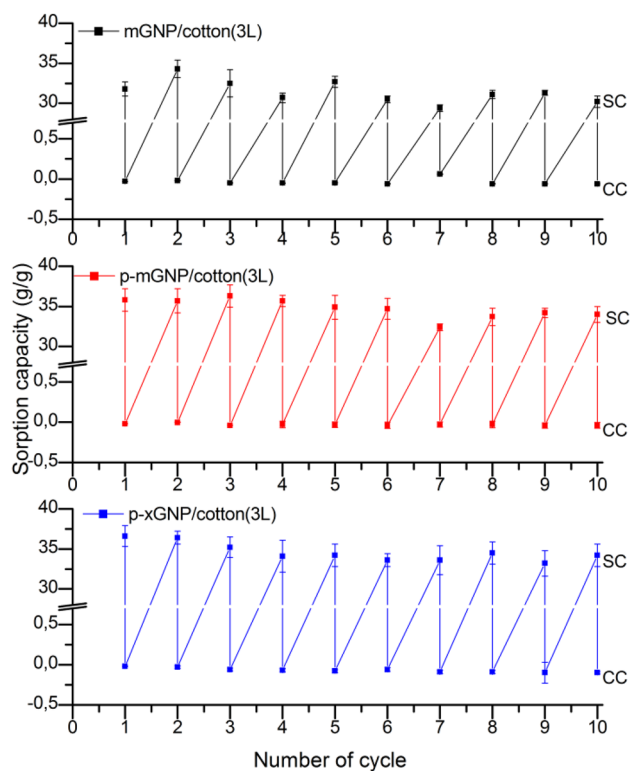


Fig. 8 Repeating sorption capacity towards ethanol and CC measurements of mGNP/cotton, pxGNP/cotton, and pmGNP/cotton

but also no significant change in sorption kinetics was observed (please see, Supplementary Materials Fig. S4b).

After evaluation of SC towards various liquids, the hydrophobized sorbents were cyclically tested to investigate the possibility of sorbent reuse. The recyclability tests were performed according to Sect. "Sorption measurements" and the results are presented in Fig. 8.

The SC of mGNP/cotton ranged from 29.4 g/g to 34.3 g/g, but no significant decrease after 10 cycles was observed. Its CC was approximately 0 g/g, which corresponds to the complete desorption of ethanol during distillation. Similar SC and CC results were observed for both pmGNP/cotton and p-xGNP/cotton. Finally, wetting by water was measured after 10 cycles. A slight decrease in θ angle was observed and it was equal $132^\circ \pm 5^\circ$, $140^\circ \pm 2^\circ$ and $136^\circ \pm 4^\circ$ for mGNP/cotton, p-mGNP/cotton and p-xGNP/cotton, respectively. Therefore, some GMs were washed out during 10 sorption cycles, but they still remained highly hydrophobic.

In addition, it is crucial for oil spill sorbents to be resilient to atmospheric conditions, such as sunlight and high humidity, thus mGNP/cotton and p-mGNP/cotton, showing the best performance, were tested for the influence of those environmental factors. After 24 h of exposure to sunlight, both mGNP/cotton and p-mGNP/cotton maintained superhydrophobic properties with a water contact angle of $131^\circ \pm 2^\circ$

and $135^\circ \pm 5^\circ$, respectively. In addition, sorption capacity towards water remained low and equal to 1.9 ± 0.4 g/g and 0.9 ± 0.2 g/g, respectively.

The samples were also resilient to humid environment. Exposure to high humidity (above 85%) for 24 h only slightly changed the wetting of mGNP/cotton and p-mGNP/cotton, resulting in a water contact angle of $133^\circ \pm 3^\circ$ and $125^\circ \pm 3^\circ$, respectively. The samples remained water repellent during soaking, resulting in a sorption capacity equal 1.1 ± 0.3 g/g and 0.8 ± 0.4 g/g, respectively.

Discussion

The presented studies are an extension of recent works about cotton sorbents coated with GO. In the majority of works GO was prepared by the Hummer's method and deposited by simple dip-coating. Then, GO/cotton was reduced to rGO/cotton and became hydrophobic. The reduction was performed either by thermal (Hoai et al. 2016; Cai et al. 2017) or hydrothermal (Ge et al. 2014; Dashairya et al. 2018) process. Moreover, Tissera et al. (Tissera et al. 2015) have shown that amphiphilic cotton may be hydrophobic even without any reduction process. The rGO/cotton samples showed θ angle ranging from 125° to 163° and SC towards organic solvents and oils 22 g/g to 55 g/g. In our previous research, we showed that not only rGO, but also mGNP can be used as hydrophobic agents (Łukawski et al. 2018b), showing the θ angle of 148° and a SC of oil of 30 g/g. Although it was possible to obtain superhydrophobic cotton sorbents with high SC towards oils (Table 2), the use of expensive GO is inhibited by its high price and massive scale of oil spills. In comparison with the other reported works, in this study,

cheap and large-scale produced GM were used as hydrophobic agents. When this work, the price of GO and rGO was still too high to meet the requirements of large-scale oil removal sorbents. The price of 1 g of GO ranged from 97 \$/g (Graphenea Inc.) to 140 \$/g (Cheaptubes Inc.), while that of rGO from 97 \$/g (Graphenea Inc.) to 190 \$/g (Cheaptubes Inc.). On the contrary, GNPs are already easily produced in large amounts at significantly lower cost. The price of 1 g of xGNP and mGNP is 0.45 \$/g and 7.3 \$/g, respectively. Despite low price, we showed that xGNP and mGNP may be used as hydrophobic agents as successfully as rGO. The presented θ angle ranged from 132° for mGNP/cotton to 142° and 148° for pyrolyzed sorbents, p-xGNP/cotton and p-mGNP/cotton, respectively. Moreover, SC was higher than in previous research and reached even 60 g/g towards chloroform (pmGNP/cotton) and 53 g/g towards motor oil (pxGNP/cotton).

GM hydrophobized cotton may have many advantages in comparison with currently used sorbents, including synthetic polymers, raw natural fibres, and inorganic materials. Synthetic polymers, such as polypropylene, have been widely used because of their high absorption capacity and ease of handling (Wei et al. 2003). However, their non-biodegradable nature and limited reusability pose significant environmental issues. Natural cellulose-based fibers, including cotton, have also been employed as sorbents in oil spill remediation. However, their hydrophilic nature results in a lack of selectivity and lower sorption capacity for oil, because they tend to absorb both water and oil (Chau et al. 2021). Inorganic sorbents, such as vermiculite (Silva et al. 2003) or sawdust (Zang et al. 2015), offer high sorption capacity but suffer from clumping and inefficient oil recovery. These materials, although used as oil sorbents, are

Table 2 Comparison of cottons hydrophobized by GM in terms of application as potential hydrophobic oil sorbents

GM/treatment	GM synthesis	Reduction process	θ [°]	SC (g/g) (oil/organic solvent)	References
Amphiphilic GO	Hummer's method	None	143	Not applicable	Tissera et al. 2015)
rGO	–	Thermal	125	Not applicable	Cai et al. 2017)
rGO	Hummer's method	Hydrothermal	151	30 (hexane) 50 (chloroform)	Ge et al. 2014)
rGO	Hummer's method	Thermal	151	23 (hexane) 45 (chloroform)	Hoai et al. 2016)
rGO	Hummer's method	Hydrothermal	163	55 (engine oil)	Dashairya et al. 2018)
rGO	Hummer's method	Hydrothermal	> 150	85–95 (crude oil)	Shiu et al. 2018)
Graphene powder	Microwave plasma synthesis	None	148	32 (chloroform) 30 (motor oil)	Łukawski et al. 2018b)
p-xGNP	Chemical exfoliation	Thermal	142 ± 8	53 (motor oil) 54 (chloroform)	This work
mGNP	Microwave plasma synthesis	None	132 ± 4	45 (motor oil) 50 (chloroform)	This work
p-mGNP	Microwave plasma synthesis	Thermal	148 ± 6	46 (motor oil) 60 (chloroform)	This work

not as hydrophobic and, therefore, as effective as graphene-coated cotton.

However, recent research efforts have focused on the development of biomimetic, nanostructured superhydrophobic biochars and aerogels. These advanced materials exhibit outstanding properties in terms of hydrophobicity, sorption capacity, and durability, surpassing those of conventional sorbents. Despite their superiority, the high cost and limitations in their synthesis currently limit their large-scale application in oil spill remediation.

Therefore, pyrolyzed graphene-coated cotton is still an interesting material that is easily scalable, inexpensive, environmentally friendly, superhydrophobic, and highly sorptive. However, it is important to note that although cotton is a natural and environmentally friendly material, the impact of graphene on marine ecosystems is still under investigation and subject to ongoing debate (Peijnenburg et al. 2015; Marchi et al. 2018; Zhao et al. 2014). All potential environmental hazards should be carefully assessed and addressed before any large-scale implementation of graphene-based sorbents for oil spill remediation.

Conclusions

Cotton roving was coated by GM materials, such as GrF, xGNP and mGNP to increase its water repellence. We found that the most important factors that influence the wetting properties are the average size of the flakes. However, the presence of defects and contaminations was also important. The mGNP material met both criteria, since it has the smallest flake size and has no contaminations containing hydrophilic groups. The material xGNP may also be used, but it requires further reduction treatment to make it hydrophobic. In addition, mGNP/cotton and xGNP/cotton may become even more hydrophobic by mild pyrolysis in vacuum. This process slightly modifies cellulose fibers and makes them less hydrophilic, therefore, improving water repellent properties. Moreover, mild pyrolysis causes an increase in SC towards organic solvents and oils.

The findings presented here offer a novel approach for the eco-friendly, cost-effective preparation of superhydrophobic sorbents for oil spill removal. However, the utility of pyrolyzed graphene-coated cotton may extend beyond this specific application, such as in the realm of oil–water separation and water filtration, although further investigations are warranted.

Supplementary Information The online version contains supplementary material available at <https://doi.org/10.1007/s13204-023-02922-2>.

Acknowledgements The authors thank the Ministry of Education and Science (Poland).

Authors' contributions DŁ participated in developing the concept and design of the study, preparing the sample, discussing the results and writing both the preliminary and final versions of the manuscript. FL was responsible for SEM imaging. MW carried out the measurements and analysis of Raman spectroscopy. AM was responsible for the search for literature and participated in the preparation of the final version of the article. AD contributed to the discussion and correction of the results.

Funding All authors certify that they have no affiliations with or involvement in any organization or entity with any financial interest or non-financial interest in the subject matter or materials discussed in this manuscript.

Data availability Raw data will be available on request.

Declarations

Conflict of interest The authors have no relevant financial or non-financial interests to disclose.

Open Access This article is licensed under a Creative Commons Attribution 4.0 International License, which permits use, sharing, adaptation, distribution and reproduction in any medium or format, as long as you give appropriate credit to the original author(s) and the source, provide a link to the Creative Commons licence, and indicate if changes were made. The images or other third party material in this article are included in the article's Creative Commons licence, unless indicated otherwise in a credit line to the material. If material is not included in the article's Creative Commons licence and your intended use is not permitted by statutory regulation or exceeds the permitted use, you will need to obtain permission directly from the copyright holder. To view a copy of this licence, visit <http://creativecommons.org/licenses/by/4.0/>.

References

- Arseneau DF (1971) Competitive reactions in the thermal decomposition of cellulose. *Can J Chem* 49(4):632–638. <https://doi.org/10.1139/v71-101>
- Belyaeva LA, Schneider GF (2020) Wettability of graphene. *Surf Sci Rep.* <https://doi.org/10.1016/j.surfrep.2020.100482>
- Bo Z, Yang Y, Chen J, Yu K, Cen K (2013) Nanoscale Plasma-enhanced chemical vapor deposition synthesis of vertically oriented graphene nanosheets. *Nanoscale* 5:5180–5204. <https://doi.org/10.1039/c3nr33449j>
- Cai G, Xu Z, Yang M, Tang B, Wang X (2017) Functionalization of cotton fabrics through thermal reduction of graphene oxide. *Appl Surf Sci* 393:441–448. <https://doi.org/10.1016/j.apsusc.2016.10.046>
- Chau MQ, Truong TT, Hoang AT, Le TH (2021) Oil spill cleanup by raw cellulose-based absorbents: a green and sustainable approach. *Energy Sources Part a: Recovery Util Environ Eff.* <https://doi.org/10.1080/15567036.2021.1928798>
- Cho E-C, Hsiao Y-S, Lee K-C, Huang J-H (2015) Few-layer graphene based sponge as a highly efficient, recyclable and selective sorbent for organic solvents and oils. *RSC Adv* 5(66):53741–53748. <https://doi.org/10.1039/c5ra06737e>
- Ciolacu D, Ciolacu F, Popa VI (2011) Amorphous cellulose - Structure and characterization. *Cellul Chem Technol* 45(1–2):13–21
- Da Silva UG, Melo MADF, Da Silva AF, De Farias RF (2003) Adsorption of crude oil on anhydrous and hydrophobized vermiculite.

- J Colloid Interface Sci 260(2):302–304. [https://doi.org/10.1016/S0021-9797\(02\)00160-1](https://doi.org/10.1016/S0021-9797(02)00160-1)
- Dashairya L, Rout M, Saha P (2018) Reduced graphene oxide - coated cotton as an efficient absorbent in oil-water separation. *Adv Comp Hybrid Mater* 1:135–148. <https://doi.org/10.1007/s42114-017-0019-9>
- De Marchi L, Pretti C, Gabriel B, Marques PAAP, Freitas R, Neto V (2018) An overview of graphene materials: Properties, applications and toxicity on aquatic environments. *Sci Total Environ*. <https://doi.org/10.1016/j.scitotenv.2018.03.132>
- Dong X, Chen J, Ma Y, Wang J, Chan-Park MB, Liu X, Wang L, Huang W, Chen P (2012) Superhydrophobic and superoleophilic hybrid foam of graphene and carbon nanotube for selective removal of oils or organic solvents from the surface of water. *Chem Commun* 48(86):10660. <https://doi.org/10.1039/c2cc35844a>
- Eckmann A, Felten A, Mishchenko A, Britnell L, Krupke R, Novoselov KS, Casiraghi C (2012) Probing the Nature of Defects in Graphene by Raman Spectroscopy. *Nano Lett* 12:3925–3930. <https://doi.org/10.1021/nl300901a>
- Ferrari AC, Basko DM (2013) Raman spectroscopy as a versatile tool for studying the properties of graphene. *Nat Nanotechnol*. <https://doi.org/10.1038/nnano.2013.46>
- Ferrari AC, Meyer JC, Scardaci V, Casiraghi C, Lazzeri M, Mauri F, Geim AK (2006) Raman spectrum of graphene and graphene layers. *Phys Rev Lett* 97(18):187401. <https://doi.org/10.1103/PhysRevLett.97.187401>
- Ge B, Zhang Z, Zhu X, Men X, Zhou X, Xue Q (2014) A graphene coated cotton for oil/water separation. *Compos Sci Technol* 102:100–105. <https://doi.org/10.1016/j.compscitech.2014.07.020>
- Gupta S, Tai N-H (2016) Carbon materials as oil sorbents: a review on the synthesis and performance. *J Mater Chem A* 4(5):1550–1565. <https://doi.org/10.1039/C5TA08321D>
- Ha H, Shanmuganathan K, Ellison CJ (2015) Mechanically stable thermally crosslinked poly(acrylic acid)/reduced graphene oxide aerogels. *ACS Appl Mater Interfaces* 7(11):6220–6229. <https://doi.org/10.1021/acsami.5b00407>
- Hoai NT, Sang NN, Hoang TD (2016) Thermal reduction of graphene-oxide-coated cotton for oil and organic solvent removal. *Mater Sci Eng, B* 216:1–6. <https://doi.org/10.1016/j.mseb.2016.06.007>
- Ji C, Zhang K, Li L, Chen X, Hu J, Yan D, Xiao G, He X (2017) High performance graphene-based foam fabricated by a facile approach for oil absorption. *J Mater Chem A* 5(22):11263–11270. <https://doi.org/10.1039/C7TA02613G>
- Kato Y, Umehara K, Aoyama M (1997a) An oil sorbent from wood fiber by mild pyrolysis. *Holz Als Roh- Und Werkstoff* 55(6):399–401. <https://doi.org/10.1007/s001070050254>
- Kato Y, Umehara K, Aoyama M (1997b) An oil sorbent from wood fiber by mild pyrolysis. *Holz als Roh-und Werkstoff* (Vol. 55).
- Kim E, Kim D, Kwak K, Nagata Y, Bonn M, Cho M (2022) Wettability of graphene, water contact angle, and interfacial water structure. *Chem* 8(5):1187–1200. <https://doi.org/10.1016/j.chempr.2022.04.002>
- Kugler S, Kowalczyk K, Spychaj T (2015) Hybrid carbon nanotubes/graphene modified acrylic coats. *Prog Org Coat* 85:1–7. <https://doi.org/10.1016/j.porgcoat.2015.02.019>
- Li R, Chen CB, Li J, Xu LM, Xiao GY, Yan DY (2014) A facile approach to superhydrophobic and superoleophilic graphene/polymer aerogels. *J Mater Chem A* 2(9):3057. <https://doi.org/10.1039/c3ta14262k>
- Lin Y, Ehlert GJ, Bukowsky C, Sodano HA (2011) Superhydrophobic functionalized graphene aerogels. *ACS Appl Mater Interfaces* 3:2200–2203. <https://doi.org/10.1021/am200527j>
- Łukawski D, Lekawa-Raus A, Lisiecki F, Koziol K, Dudkowiak A (2018a) Towards the development of superhydrophobic carbon nanomaterial coatings on wood. *Prog Org Coat* 125:23–31. <https://doi.org/10.1016/j.porgcoat.2018.08.025>
- Łukawski D, Lisiecki F, Dudkowiak A (2018b) Coating cellulosic materials with graphene for selective absorption of oils and organic solvents from water. *Fibers and Polymers* 19(3):524–530. <https://doi.org/10.1007/s12221-018-7879-7>
- Lv P, Almeida G, Perré P (2012) Torrefaction of cellulose: Validity and limitation of the temperature/duration equivalence. *BioResources* 7(3):3720–3731. <https://doi.org/10.15376/biores.7.3.3720-3731>
- Lv LB, Cui TL, Zhang B, Wang HH, Li XH, Chen JS (2015a) Wrinkled graphene monoliths as superabsorbing building blocks for superhydrophobic and superhydrophilic surfaces. *Angew Chem Int Ed* 54(50):15165–15169. <https://doi.org/10.1002/anie.201507074>
- Lv P, Almeida G, Perré P (2015b) TGA-FTIR analysis of torrefaction of lignocellulosic components (cellulose, xylan, lignin) in isothermal conditions over a wide range of time durations. *BioResources* 10(3):4239–4251. <https://doi.org/10.15376/biores.10.3.4239-4251>
- Malesevic A, Vitchev R, Schouteden K, Volodin A, Zhang L, Tendeloo G, Vanhulsel A, Van Haesendonck C (2008) Synthesis of few-layer graphene via microwave plasma-enhanced chemical vapour deposition. *Nanotechnology* 19(30):305604. <https://doi.org/10.1088/0957-4484/19/30/305604>
- Nguyen DD, Tai N-H, Lee S-B, Kuo W-S (2012) Superhydrophobic and superoleophilic properties of graphene-based sponges fabricated using a facile dip coating method. *Energy Environ Sci* 5(7):7908. <https://doi.org/10.1039/c2ee21848h>
- Oliveira LMTM, Saleem J, Bazargan A, da Duarte JLS, McKay G, Meili L (2021) Sorption as a rapidly response for oil spill accidents: a material and mechanistic approach. *J Hazard Mater*. <https://doi.org/10.1016/j.jhazmat.2020.124842>
- Oribayo O, Feng X, Rempel GL, Pan Q (2017) Synthesis of lignin-based polyurethane/graphene oxide foam and its application as an absorbent for oil spill clean-ups and recovery. *Chem Eng J* 323:191–202. <https://doi.org/10.1016/j.cej.2017.04.054>
- Peijnenburg WJGM, Baalousha M, Chen J, Chaudry Q, Von Der Kammer F, Kuhlbusch TAJ, Lead J, Nickel C, Quik J, Renker M, Wang Z, Koelmans AA (2015) A review of the properties and processes determining the fate of engineered nanomaterials in the aquatic environment. *Crit Rev Environ Sci Technol* 45(19):2084–2134. <https://doi.org/10.1080/10643389.2015.1010430>
- Rytel K, Widelicka M, Łukawski D, Lisiecki F, Kędzierski K, Wróbel D (2018) Ultrasonication-induced sp³ hybridization defects in Langmuir-Schaefer layers of turbostratic graphene. *Phys Chem Chem Phys* 20(18):12777–12784. <https://doi.org/10.1039/c8cp01363b>
- Saha P, Dashairya L (2018) Reduced graphene oxide modified melamine formaldehyde (rGO@MF) superhydrophobic sponge for efficient oil-water separation. *J Porous Mater* 4:1475–1488. <https://doi.org/10.1007/s10934-018-0560-0>
- Shateri-Khalilabad M, Yazdanshenas ME (2013) Preparation of superhydrophobic electroconductive graphene-coated cotton cellulose. *Cellulose* 20(2):963–972. <https://doi.org/10.1007/s10570-013-9873-y>
- Shen J, Hu Y, Li C, Qin C, Ye M (2009) Synthesis of amphiphilic graphene nanoplatelets. *Small* 4(1):82–85. <https://doi.org/10.1002/sml.200800988>
- Shiu RF, Lee CL, Hsieh PY, Chen CS, Kang YY, Chin WC, Tai NH (2018) Superhydrophobic graphene-based sponge as a novel sorbent for crude oil removal under various environmental conditions. *Chemosphere* 207:110–117. <https://doi.org/10.1016/j.chemosphere.2018.05.071>
- Singh E, Chen Z, Houshmand F, Ren W, Peles Y, Cheng HM, Koratkar N (2013) Superhydrophobic graphene foams. *Small* 9(1):75–80. <https://doi.org/10.1002/sml.201201176>
- Some S, Kim Y, Yoon Y, Yoo H, Lee S, Park Y, Lee H (2013) High-Quality Reduced Graphene Oxide and Healing Process. *Sci Rep* 3(1929):1–5. <https://doi.org/10.1038/srep01929>

- Stalder AF, Kulik G, Sage D, Barbieri L, Hoffmann P (2006) A snake-based approach to accurate determination of both contact points and contact angles. *Colloids Surf, A* 286(1–3):92–103. <https://doi.org/10.1016/j.colsurfa.2006.03.008>
- Su X, Li H, Lai X, Zhang L, Wang J, Liao X, Zeng X (2017) Vapor–Liquid Sol–Gel Approach to Fabricating Highly Durable and Robust Superhydrophobic Polydimethylsiloxane@Silica Surface on Polyester Textile for Oil–Water Separation. *ACS Appl Mater Interfaces* 9:28089–28099. <https://doi.org/10.1021/acsami.7b08920>
- Tissera ND, Wijesena RN, Perera JR, De Silva KMN, Amaratunge GAJ (2015) Hydrophobic cotton textile surfaces using an amphiphilic graphene oxide (GO) coating. *Appl Surf Sci* 324:455–463. <https://doi.org/10.1016/j.apsusc.2014.10.148>
- Viculis LM, Mack JJ, Mayer OM, Thomas H, Kaner RB (2005) Intercalation and exfoliation routes to graphite nanoplatelets. *J Mater Chem* 15:974–978. <https://doi.org/10.1039/b413029d>
- Wang JN, Zhang YL, Liu Y, Zheng W, Lee LP, Sun HB (2015) Recent developments in superhydrophobic graphene and graphene-related materials: From preparation to potential applications. *Nanoscale*. <https://doi.org/10.1039/c5nr00719d>
- Wei QF, Mather RR, Fotheringham AF, Yang RD (2003) Evaluation of nonwoven polypropylene oil sorbents in marine oil-spill recovery. *Mar Pollut Bull* 46(6):780–783. [https://doi.org/10.1016/S0025-326X\(03\)00042-0](https://doi.org/10.1016/S0025-326X(03)00042-0)
- Xu L, Xiao G, Chen C, Li R, Mai Y, Sun G, Yan D (2015) Superhydrophobic and superoleophilic graphene aerogel prepared by facile chemical reduction. *J Mater Chem A* 3(14):7498–7504. <https://doi.org/10.1039/C5TA00383K>
- Zang D, Liu F, Zhang M, Gao Z, Wang C (2015) Novel superhydrophobic and superoleophilic sawdust as a selective oil sorbent for oil spill cleanup. *Chem Eng Res Des* 102:34–41. <https://doi.org/10.1016/j.cherd.2015.06.014>
- Zhao J, Wang Z, White JC, Xing B (2014) Graphene in the aquatic environment: Adsorption, dispersion, toxicity and transformation. *Environ Sci Technol* 48(17):9995–10009. <https://doi.org/10.1021/es5022679>

Publisher's Note Springer Nature remains neutral with regard to jurisdictional claims in published maps and institutional affiliations.